line-shape analysis gives additional confidence in the phenylene dynamics picture as outlined here. It should be noted that due to the increased quadrupolar interaction, the features that distinguish homogeneous and inhomogeneous line shapes for intermediate rates, i.e., the differences at the absorption maxima, are enhanced over the CSA case as shown in Figure 9.

Acknowledgment. This research was carried out with the financial support of National Science Foundation Grant DMR-790677, of National Science Foundation Equipment Grant No. CHE 77-09059, of National Science Foundation Grant No. DMR-8018679, and of U.S. Army Research Office Grants DAAG 29-82-G-0001 and DAAG 29 85-K0126.

Registry No. BPA-PC (copolymer), 25037-45-0; BPA-PC (SRU), 24936-68-3.

References and Notes

(1) O'Gara, J. F.; Jones, A. A.; Hung, C.-C.; Inglefield, P. T. *Macromolecules* **1985**, *18*, 1117.
(2) Spiess, H. W. *Advances in Polymer Science*; Kausch, H. H., Zachmann, H. G., Eds.; Springer-Verlag: Berlin, 1984.
(3) (a) Illers, K.; Bruer, H. *Kolloid-Z.* **1961**, *176*, 110. (b) Krum, F.; Muller, F. H. *Kolloid-Z.* **1957**, *164*, 81. (c) Krum, F. *Kolloid-Z.* **1959**, *165*, 77.
(4) Yee, A. F.; Smith, S. A. *Macromolecules* **1981**, *14*, 54.
(5) Jones, A. A. *Macromolecules* **1985**, *18*, 902.
(6) Wemmer, D. E. Ph.D. Thesis, University of California, Berkeley, CA, 1979.
(7) Roy, A. K.; Jones, A. A.; Inglefield, P. T. *J. Magn. Reson.* **1985**, *64*, 441.
(8) Ngai, K. L. *Comments Solid State Phys.* **1979**, *9*, 127.
(9) Ngai, K. L.; White, C. T. *Phys. Rev. B* **1979**, *20*, 2476.
(10) Ngai, K. L. *Phys. Rev. B* **1980**, *22*, 2066.
(11) (a) Schaefer, J.; Stejskal, E. O.; Steger, T. R.; Sefcik, M. D.; McKay, R. A. *Macromolecules* **1980**, *13*, 1121. (b) Steger, T. R.; Schaefer, J.; Stejskal, E. O.; McKay, R. A. *Macromolecules* **1980**, *13*, 1127.
(12) Kaplan, J. I.; Garroway, A. N. *J. Magn. Reson.* **1982**, *49*, 464.
(13) Mehring, M. *High Resolution NMR in Solids*, 2nd ed.; Springer-Verlag: New York, 1983.
(14) Bloembergen, N.; Rowland, T. J. *Acta Metall.* **1955**, *1*, 731.
(15) Wemmer, D. E.; Ruben, D. J.; Pines, A. *J. Am. Chem. Soc.* **1981**, *103*, 28.
(16) Williams, G.; Watts, D. C. *Trans. Faraday Soc.* **1970**, *66*, 80.
(17) Montroll, E. W.; Bendler, J. T. *J. Stat. Phys.* **1984**, *34*, 129.
(18) Bendler, J. T.; Shlesinger, M. F. In *Studies in Statistical Mechanics*; Shlesinger, M. F., Weiss, G. H., Eds.; North-Holland: New York, 1985; Vol. 12.
(19) Connolly, J.; Jones, A. A.; Inglefield, P. T., to be published.
(20) Shlesinger, M. F.; Montroll, E. W. *Proc. Natl. Acad. Sci. U.S.A.* **1984**, *81*, 1280.
(21) Shlesinger, M. F. *J. Stat. Phys.* **1984**, *36*, 639.
(22) Blumen, A.; Zumofen, G.; Klafter, J. *Phys. Rev. B* **1984**, *30*, 5379.

Surface Structure and Oxygen Permeation in Mixed Multibilayer Films of Hydrocarbon and Fluorocarbon Amphiphiles

Nobuyuki Higashi,† Toyoki Kunitake,*† and Tisato Kajiyama‡

Department of Organic Synthesis and Department of Applied Chemistry, Faculty of Engineering, Kyushu University, Fukuoka 812, Japan. *Received August 29, 1985*

ABSTRACT: Multicomponent bilayers of double-chain (fluorocarbon, 2F; hydrocarbon, 2H; mixed chain, 1F1H) ammonium amphiphiles were immobilized on Millipore membranes as composite films with poly(vinyl alcohol). Differential scanning calorimetry and ESCA indicated that the hydrocarbon and fluorocarbon components form separated domains and that the fluorocarbon component is concentrated near the film surface. Permeation of O_2 and N_2 through these films was examined by the high-vacuum method. The separation factor (P_{O_2}/P_{N_2} = 2.0–2.8) was apparently determined by the surface monolayer formed from the fluorocarbon (2F) amphiphile, without regard to the hydrocarbon (2H) content. The permeability coefficient (P) was enhanced by the presence of the fluid domain of the liquid-crystalline hydrocarbon (2H) bilayer, and a 100 times jump in P was observed for a composite film of 2F/2H/1F1H (1:7:1) and PVA near the phase transition temperature of the hydrocarbon bilayer.

Introduction

Aqueous bilayer membranes can be immobilized by casting on glass in the form of transparent films that maintain the bilayer characteristics.[1-4] Fluorocarbon bilayer films obtained by casting with and without poly(vinyl alcohol) (PVA) exhibit the oxygen-enrichment property.[5] Takahara et al.[6] conducted the structural characterization of composite films of PVA and fluorocarbon bilayer membranes by X-ray diffraction and X-ray photoelectron spectroscopy (XPS) and discovered that the fluorocarbon bilayer lamella is spontaneously concentrated at the film surface with the bilayer orientation parallel to the film plane.

In general, permeability coefficients of the bilayer membrane are enhanced when the bilayer membrane is in the liquid-crystalline phase rather than in the crystalline phase. Fluorocarbon bilayer films show enhanced oxygen permeation due to the affinity between fluorocarbon moieties and molecular oxygen. In contrast, fluorocarbon bilayers possess high phase transition temperatures (T_c), and the enhanced permeation due to the liquid-crystalline state cannot be achieved at ambient temperatures. We

Chart I

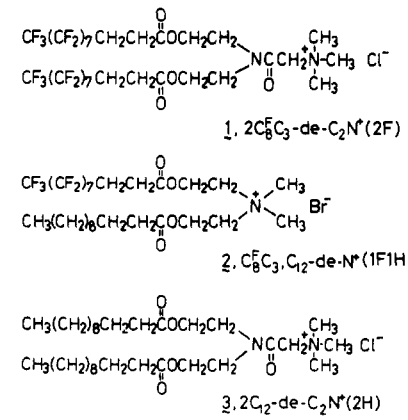

† Department of Organic Synthesis, Contribution No. 804.
‡ Department of Applied Chemistry.

0024-9297/86/2219-1362$01.50/0

Chart II

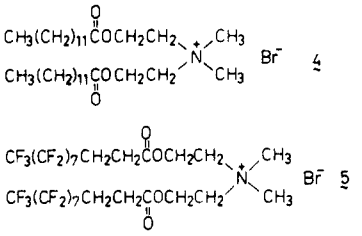

therefore intended to combine oxygen affinity of the fluorocarbon bilayer and enhanced permeation through the liquid-crystalline hydrocarbon bilayer. Fluorocarbon and hydrocarbon bilayers are not readily miscible,[7,8] and their composite bilayers may exhibit advantages of both of the component bilayers.

In the present study, we prepared cast films of multicomponent bilayers of the amphiphiles shown in Chart I and examined their component distribution and gas permeation characteristics.

Experimental Section

Materials. The preparations of $2C^F_8C_3$-de-C_2N^+ (2F),[9] $C^F_8C_3$, C_{12}-de-N^+2C_1 (1F1H),[7] and $2C_{12}$-de-C_2N^+ (2H)[9] have been described elsewhere. PVA employed possesses an average molecular weight of 1.5×10^{-5} and a saponification value of 98.1%.

Cast bilayer films were prepared as follows. Given amounts of amphiphiles were dissolved in $CHCl_3$. After $CHCl_3$ was removed by evaporation, the thin-film residues were dispersed in deionized water by sonication. The dispersions were mixed with aqueous PVA with careful stirring and were cast on glass Petri dishes at room temperature. Transparent films (thickness, 20–35 μm) were obtainable after vacuum-drying. The combined fraction of the bilayer components was always 70 wt %, and the bilayer compositions (in molar ratios) were set at 1:1 and 1:2 (2F/2H) for the two-component systems and at 1:1:1, 1:5:1, and 1:7:1 (2F/2H/1F1H) for the three-component systems.

Differential Scanning Calorimetry (DSC). Bilayer films were cut into small pieces and placed in Ag sample pans. The measurement was started from 0 to 100 °C at a heating rate of 2 °C/min with a Seiko Electronics SSC/560 instrument. The detailed procedure is given elsewhere.[10]

X-ray Photoelectron Spectroscopy (XPS). XPS spectra were obtained at 8 kV and 30 mA with an ESCA 750 photoelectron spectrometer (Shimadzu Co., Ltd.). The charging shift was corrected with the C_{1s} line emitted from neutral hydrocarbon.

Gas Permeation. The permeation rates of O_2 and N_2 were measured by the high-vacuum method[11] at 20–80 °C. The gas pressure at the upstream side was kept constant (40 cmHg), and the pressure increase in the downstream side was determined by a McLeod gage at given time intervals.

Results and Discussion

Phase Separation of Bilayer in Multicomponent Films. Phase separation of hydrocarbon (4) and fluorocarbon (5) bilayers, shown in Chart II, in aqueous dispersions has been investigated by differential scanning calorimetry and by the fluorescence probe method.[7] These hydrocarbon and fluorocarbon bilayers remained phase-separated in mixed-bilayer vesicles; however, addition of a mixed-chain amphiphile (2, 1F1H) produced a seemingly homogeneous bilayer, as inferred from DSC data. A more complicated situation arises in bilayer mixtures of triple-chain ammonium amphiphiles in which the number of the fluorocarbon chain is changed from zero to three.[8]

Similar results were obtained for aqueous mixtures of 1, 2, and 3 in the present study. Figure 1 displays DSC thermograms of aqueous bilayer dispersions and cast bilayer–PVA films. In aqueous dispersions of 1 (2F) and 3 (2H), the DSC peaks are located at 75 and 21 °C, respectively. An equimolar mixture of these amphiphiles

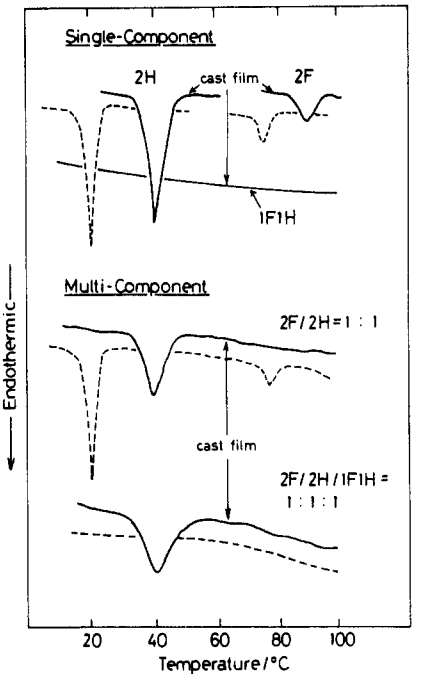

Figure 1. DSC thermograms of multibilayer composite films and aqueous bilayer dispersions: (solid line) cast bilayer film; (dotted line) aqueous bilayer dispersion.

gives a completely phase-separated bilayer, since its DSC thermogram is a simple sum of the two one-component thermograms. The DSC peaks completely disappear when an equimolar amount of 2 (1F1H) is added as a third component. In the PVA composite films of 1 (2F) and 3 (2H), DSC peaks are shifted toward higher temperatures (89 and 40 °C, respectively) than those of the corresponding aqueous dispersions. The increase in T_c in cast films has been observed commonly in other systems.[1-4]

A two-component composite film (2F/2H–PVA; molar ratio, 2F/2H = 1:1) gives a DSC peak at 39 °C, in close agreement with that (40 °C) of the single-component composite film (2F–PVA). A DSC peak was found at the same temperature for a two-component composite film of a different molar ratio (2F/2H–PVA; molar ratio, 2F/2H = 1:2). These data indicate the presence of 2H bilayer domains in the film. In contrast, the peak due to the 2F component is not found at ca. 89 °C, unlike in the case of an aqueous 2F/2H dispersion. The 2H peak for the cast film is broadened relative to that for the aqueous dispersion, and the 2F peak is much smaller than the 2H peak (the enthalpy changes for the aqueous bilayers are 0.5 and 12.8 kcal/mol, respectively). These features make detection of the 2F peak less feasible. We believe, in spite of the lack of the 2F peak, that phase separation of 2F and 2H components is appreciable in the composite film as in the aqueous dispersion.

Three-component composite films (2F/2H/1F1H–PVA) give DSC peaks at 38–41 °C, in contrast with their aqueous dispersions (no DSC peaks). The location of the peak changes only slightly with the variation in the amphiphile composition and agrees with T_c of the 2H–PVA composite film. It is clear that the hydrocarbon component (2H) forms separate domains from those of the fluorocarbon (2F) and mixed-chain (1F1H) components.

Surface Structure. The elemental composition of the film surface was examined by XPS analysis. Figure 2 shows the C_{1s} and F_{1s} spectra of a cast film of 2F/2H (1:2)–PVA. In order to examine the depth profile of the elemental composition, the takeoff angle θ of the photoemitted electron was set at 15°, 30°, 45°, and 90°. The

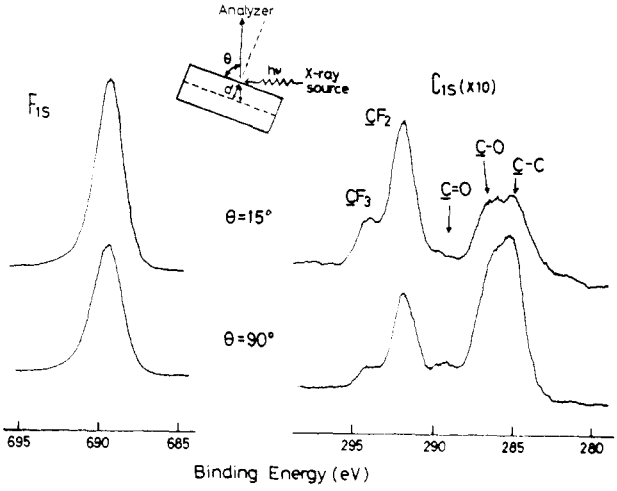

Figure 2. X-ray photoelectron spectra of C_{1s} and F_{1s} of a 2F/2H (1:2)–PVA film.

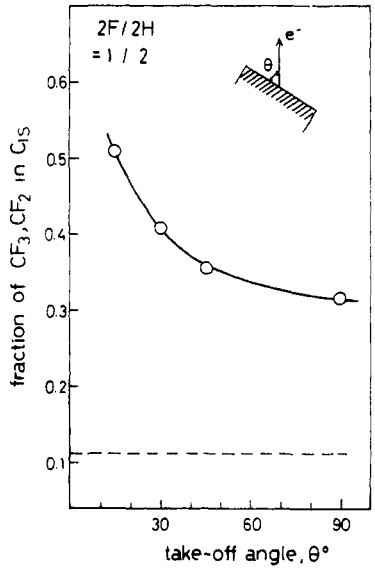

Figure 3. Depth profile of the fraction of CF_3 and CF_2 in total C_{1s} for a 2F/2H (1:2)–PVA film.

insert in Figure 2 illustrates the relation between the incident X-ray beam and the photoemitted electron. The sampling depth, d, is proportional to the mean free path of the photoelectron in the sample and to sin θ.[12] Figure 2 contains two spectra at $\theta = 15°$ and 90°. Both spectra are composed of five C_{1s} peaks and one F_{1s} peak, in addition to O_{1s} and N_{1s} peaks (not shown in the figure). The C_{1s} peaks at 285.0, 286.5, and 288.8 eV are assigned respectively to neutral carbon, ethereal carbon, and carbonyl carbon. The two C_{1s} peaks at 292.7 and 294.5 eV are attributed to CF_2 and CF_3, respectively. The intensity of these peaks relative to that of the total C_{1s} peak is a measure of the concentration of the fluorocarbon components. The relative intensity clearly changes with the takeoff angle.

Figures 3 and 4 show the relation between the takeoff angle and the fraction of the CF_2 and CF_3 units in the total carbon, as estimated from the relative peak intensity. The sampling depth increases with increasing takeoff angles, being approximately 12 Å at $\theta = 15°$ and 45 Å at $\theta = 90°$. The fluorocarbon fraction increases with decreasing takeoff angles in both the two-component film (Figure 3) and the three-component film (Figure 4), indicating that the fluorocarbon components are concentrated near the film surface. The fraction at $\theta = 15°$ is 0.508 for the 2F/2H–

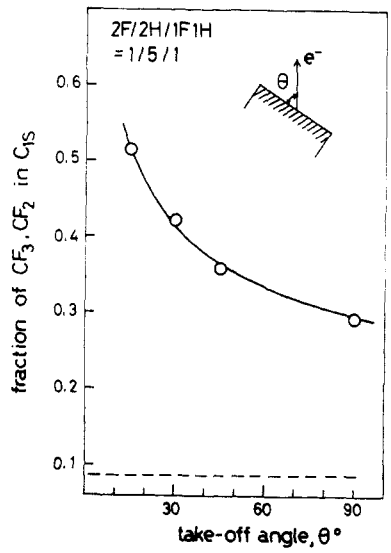

Figure 4. Depth profile of the fraction of CF_3 and CF_2 in total C_{1s} for a 2F/2H/1F1H (1:5:1)–PVA film.

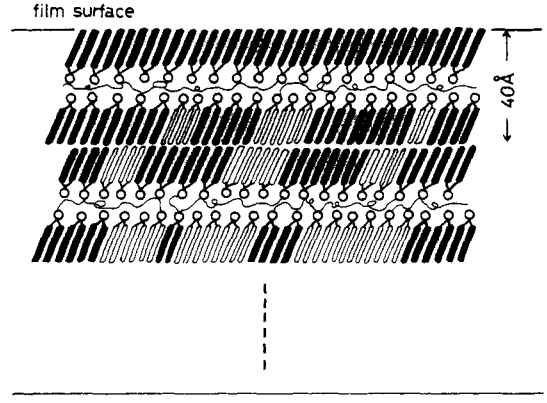

Figure 5. Schematic illustration of a multicomponent bilayer film.

PVA film and 0.511 for the 2F/2H/1F1H–PVA film. These values are virtually identical with that (0.516) of a pure 2F film. Since the sampling depth in this case is approximately 12 Å (7.5–15 Å)[13] and the monolayer depth is ca. 20 Å (see below), these results strongly suggest that the film surface is composed completely of the monolayer of the double fluorocarbon tailed amphiphile (2F). The mixed-chain component (1F1H) is not included in the surface monolayer.

As the sampling depth becomes deeper, the fluorocarbon fraction decreases. However, the values are much larger than those calculated for homogeneously mixed films: 0.111 for the 2F/2H–PVA films and 0.079 for the 2F/2H/1F1H–PVA film. Thus, the fluorocarbon components are concentrated even at the depth of 30–60 Å ($\theta = 90°$).[13] These situations are illustrated schematically in Figure 5.

As mentioned above, the DSC data indicate that phase separation is promoted in a cast film. The XPS data can provide an explanation for it at least partially. The surface monolayer plays a crucial role in the casting process. The fluorocarbon monolayer is formed preferentially in the initial stage of the casting process because of its lower surface energy relative to that of the hydrocarbon monolayer. This would promote the subsequent growth of the fluorocarbon layer from the surface, leaving the hydrocarbon component (and PVA) behind. The enhanced phase separation observed in the DSC study is produced by the selective formation of the fluorocarbon layer near the film surface, in addition to the tendency for formation

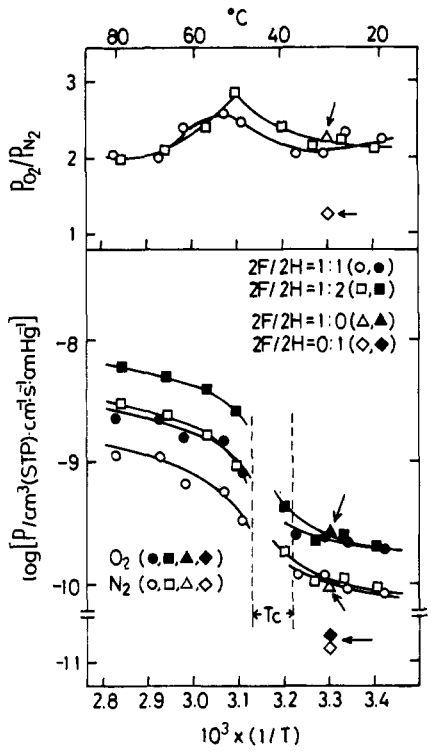

Figure 6. Temperature dependence of permeability coefficient (P) and separation factor (P_{O_2}/P_{N_2}) for 2F/2H–PVA films. Data for 2F–PVA and 2H–PVA films are denoted by arrows.

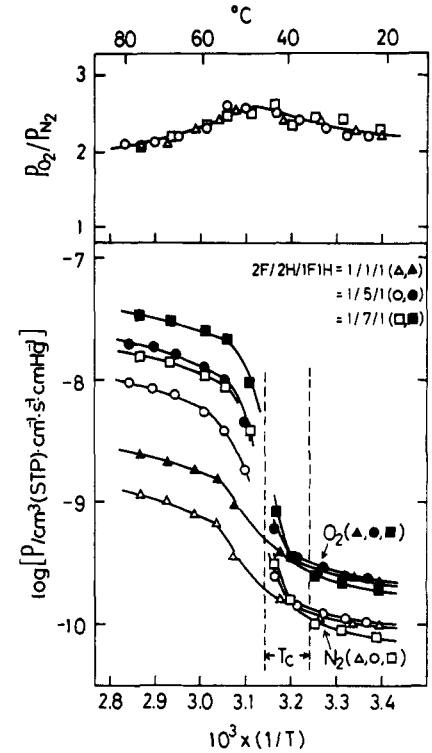

Figure 7. Temperature dependences of permeability coefficient (P) and separation factor (P_{O_2}/P_{N_2}) for the 2F/2H/1F1H–PVA films.

of separate domains within a bilayer.

Concentration of a fluorocarbon amphiphile near the film surface has been observed for 2F–PVA composite films by Takahara and others.[6] They prepared 2F–PVA-cast films of varied compositions (2F content, 19–83 wt %) and conducted the X-ray diffraction and XPS studies. The diffraction pattern in the film edge suggested the presence of the 2F lamellae parallel to the film plane. The ordered structure was present in the cast film with the lowest 2F content. The observed long spacing indicates that the 2F amphiphiles are packed in the lamellar bilayer at an angle of 30° against the film plane. The XPS analysis data of the 2F–PVA film indicated that the fluorocarbon monolayer is formed at the film surface.

Apparently, incorporation of the hydrocarbon component as in the present study does not interfere with the formation of the fluorocarbon monolayer at the surface.

Gas Permeation. Figure 6 exhibits temperature dependences of the permeability coefficient (P_{O_2} and P_{N_2}) and the separation factor ($\alpha = P_{O_2}/P_{N_2}$) for 2F/2H–PVA composite films. At temperatures below T_c of the hydrocarbon component (2H), the P values are not affected by the content of the fluorocarbon component, being in the range of 10^{-9}–10^{-10} cm^3 (STP) cm^{-1}·s^{-1}·cmHg^{-1}. The permeation data for simpler composite films at 30 °C are also given in the figure. In the case of a 2F (70 wt %)–PVA film, both the P_{O_2} and P_{N_2} values are close to those of the 2F/2H–PVA film, and the values for a 2H(50 wt %)–PVA film (uniform films were not obtainable at higher 2H content) are roughly an order of magnitude smaller. Gas permeability is undoubtedly enhanced by the presence of the 2F layer.

The P values of 2F/2H–PVA film are greatly enhanced in the T_c region and level off at higher temperatures. The extent of the drastic increase is enhanced with increasing contents of the hydrocarbon component: ca. 20 times enhancement in P for a cast film with 2F/2H = 1:2. The enhanced fluidity of the 2H bilayer domain is responsible for the P jump, since the 2F component does not show phase transition behavior in these temperature ranges. Unfortunately, a homogeneous cast film could not be obtained at higher 2H contents, and further enhancement in P at $T > T_c$ was not attained in the 2F/2H–PVA system.

The separation factor α changes little with the change in the component composition. Maximal values (α = 2.7–2.9) are attained at the higher end of the T_c region and become smaller at higher and lower temperatures. The α values for the 2F–PVA film and the 2H–PVA film are 2.3 and 1.3, respectively, at 30 °C. It is clear that the large α values observed for the 2F/2H–PVA films arise from the presence of the 2F layer.

A wider variation of the component composition was possible with 2F/2H/1F1H composite films. Figure 7 gives the results. The temperature dependence of P is similar to those observed for the 2F/2H–PVA film. The P values (for O_2 and N_2) are virtually unaffected by the component composition at temperatures below T_c of the 2H bilayer, but are greatly enhanced at the higher end of the T_c region (indicated by the two dotted lines in Figure 7). The extent of the P jump again increases with increasing contents of the hydrocarbon component, being ca. 100 times for a PVA composite film of 2F/2H/1F1H (1:7:1). The extent of the P jump is reduced to 10 times when the amount of the hydrocarbon component is decreased (2F/2H/1F1H = 1:1:1). The permeability experiment was also conducted for a 1F1H(70 wt %)–PVA film. The log P value linearly decreased with $1/T$, α being 1.3–1.4. These results clearly show that gas permeation is promoted by the presence of the fluid, liquid-crystalline phase of the 2H bilayer. The separation factor again showed a maximum at the higher end of T_c and was insensitive to the bilayer composition.

Kajiyama and co-workers[14-17] carried out the permeation experiment by using composite membranes of polymer (poly(vinyl chloride)) and thermotropic liquid crystal (EBBA: *N*-(4-ethoxybenzylidene)-4′-butylaniline). The liquid crystal forms continuous phases in the polymer matrix, and the P value is enhanced by factors of 20–30

by the temperature change of a few degrees near T_c of the liquid crystal. The viscosity of the nematic phase of EBBA is in the same range as that of liquid water, and the liquid-crystalline domain supposedly acts as the efficient mobile region of the gases. It was concluded by these authors that the temperature dependence of P is influenced by the thermal motion of the membrane component as well as by the continuity and/or size of the liquid-crystal phase.

An analogous argument may be presented for interpretation of the permeation characteristics of the multicomponent bilayer film. Discontinuous jump of P at T_c is ascribable to greater gas mobility in the liquid-crystalline phase of the hydrocarbon component, and the jump becomes larger as the hydrocarbon domain is enlarged.

Concluding Remarks

Multicomponent bilayer membranes can be immobilized in the form of PVA composite films. The DSC and XPS data indicate that the hydrocarbon and fluorocarbon bilayer components are phase-separated and that the fluorocarbon component is concentrated near the film surface. These component distributions produce favorable effects on permselectivity of O_2 gas. The selectivity (P_{O_2}/P_{N_2}) is apparently determined by the surface monolayer (or layers close to the surface) of the fluorocarbon component, and the permeability is promoted by the presence of large domains of the fluid (in the liquid-crystalline state) hydrocarbon bilayer.

Acknowledgment. We extend our appreciation to the Asahi Glass Foundation for Industrial Technology for financial support.

Registry No. 1, 91362-66-2; 2, 89373-65-9; 3, 100993-84-8; 4, 100993-85-9; 5, 82838-66-2; O_2, 7782-44-7; N_2, 7727-37-9.

References and Notes

(1) Nakashima, N.; Ando, R.; Kunitake, T. *Chem. Lett.* **1983**, 1577.
(2) Shimomura, M.; Kunitake, T. *Polym. J. (Tokyo)* **1984**, *16*, 187.
(3) Higashi, N.; Kunitake, T. *Polym. J. (Tokyo)* **1984**, *16*, 583.
(4) Kunitake, T.; Tsuge, A.; Nakashima, N. *Chem. Lett.* **1984**, 1783.
(5) Kunitake, T.; Higashi, N.; Kajiyama, T. *Chem. Lett.* **1984**, 717.
(6) Takahara, A.; Kajiyama, T., personal communication.
(7) Kunitake, T.; Tawaki, S.; Nakashima, N. *Bull. Chem. Soc. Jpn.* **1983**, *56*, 3235.
(8) Kunitake, T.; Higashi, N. *J. Am. Chem. Soc.* **1985**, *107*, 692.
(9) Kunitake, T.; Asakuma, S.; Higashi, N.; Nakashima, N. *Rep. Asahi Glass Found. Ind. Technol.* **1984**, *45*, 163.
(10) Okahata, Y.; Ando, R.; Kunitake, T. *Ber. Bunsen-Ges. Phys. Chem.* **1981**, *85*, 789.
(11) Barrer, R. M.; Skirrow, G. *J. Polym. Sci.* **1948**, *3*, 549.
(12) Hoffman, S. "Depth Profiling" in *Practical Surface Analysis*; Briggs, D.; Seak, M. P., Eds.; Wiley: New York, 1983.
(13) Brundle, C. R. *J. Vac. Sci. Technol.* **1974**, *11*, 212.
(14) Kajiyama, T.; Nagata, Y.; Washizu, S.; Takayanagi, M. *J. Membr. Sci.* **1982**, *11*, 39.
(15) Kajiyama, T.; Washizu, S.; Takayanagi, M. *J. Appl. Polym. Sci.* **1984**, *29*, 3955.
(16) Washizu, S.; Terada, I.; Kajiyama, T.; Takayanagi, M. *Polym. J. (Tokyo)* **1984**, *16*, 307.
(17) Kajiyama, T.; Washizu, S.; Ohmori, Y. *J. Membr. Sci.* **1985**, *24*, 73.

Phase Equilibria in Rodlike Systems with Flexible Side Chains†

M. Ballauff

Max-Planck-Institut für Polymerforschung, 65 Mainz, FRG. *Received July 31, 1985*

ABSTRACT: The lattice theory of the nematic state as given by Flory is extended to systems of rigid rods of axial ratio x and appended side chains characterized by the product of z, the number of side chains per rod, and m, the number of segments per side chain. Soft intermolecular forces are included by using the familiar interaction parameter. Special attention is paid to the form of the orientational distribution function, which is introduced in terms of the refined treatment devised by Flory and Ronca as well as in its approximative form given by Flory in 1956. At nearly athermal conditions the theory presented herein predicts a narrowing of the biphasic gap with increasing volume fraction of the side chains. The region where two anisotropic phases may coexist becomes very small in the presence of side chains. It is expected to vanish at a certain critical volume ratio of side chains and rigid core of the polymer molecule. The dense anisotropic phase at equilibrium with a dilute isotropic phase at strong interactions between the solute particles (wide biphasic region) is predicted to become less concentrated with increase of the product of z and m. The deductions of the treatment presented herein compare favorably with results obtained on lyotropic solutions of helical polypeptides like poly(γ-benzyl glutamate).

During recent years there has been a steadily growing interest in thermotropic and lyotropic polymers. Spinning or injection molding in the liquid-crystalline state can lead to fibers of high strength and stiffness.[1] However, the melting point of typical aromatic polyesters exhibiting a mesophase often exceeds 500 °C,[2] which makes the processing of these materials by conventional methods very difficult. In order to reduce the melting temperature of thermotropic polymers, flexible spacers have been inserted between the mesogenic units.[3] But these semiflexible polymers no longer possess the rigidity necessary to produce the desirable mechanical properties.[4] Alternatively, sufficient solubility and lower melting point may be achieved by appending flexible side chains to rigid rod polymers. This third type of liquid-crystalline polymer has been the subject of a number of recent studies. Lenz and co-workers showed that substitution with linear or branched alkyl chains[5,6] considerably lowers the melting point of poly(phenylene terephthalate). Similar observations have been made in the course of a study of poly(3-*n*-alkyl-4-hydroxybenzoic acids).[7] Gray and co-workers demonstrated that side-chain-modified cellulose derivatives exhibit thermotropic as well as lyotropic behavior.[8,9] The solution properties of poly(γ-benzyl glutamates) (PBLG) are directly influenced by the presence of flexible side chains, as has been pointed out by Flory and Leonard.[10] The thermodynamics of PBLG in various solvents has been investigated theoretically as well as experimentally by Miller and co-workers,[11,12] leading to the conclusion

† Dedicated to the memory of Professor P. J. Flory.

0024-9297/86/2219-1366$01.50/0